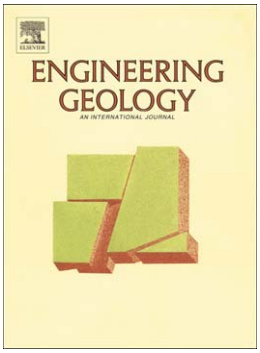

Analysis of notch effect on the fracture behaviour of granite and limestone: An approach from the Theory of Critical Distances

S. Cicero, T. García, J. Castro, V. Madrazo, D. Andrés

PII: S0013-7952(14)00103-3
DOI: doi: 10.1016/j.enggeo.2014.05.004
Reference: ENGEO 3785

To appear in: *Engineering Geology*

Received date: 2 January 2014
Revised date: 7 April 2014
Accepted date: 13 May 2014

Please cite this article as: Cicero, S., García, T., Castro, J., Madrazo, V., Andrés, D., Analysis of notch effect on the fracture behaviour of granite and limestone: An approach from the Theory of Critical Distances, *Engineering Geology* (2014), doi: 10.1016/j.enggeo.2014.05.004

ANALYSIS OF NOTCH EFFECT ON THE FRACTURE BEHAVIOUR OF GRANITE AND LIMESTONE: AN APPROACH FROM THE THEORY OF CRITICAL DISTANCES

S. Cicero[a], T. García[a], J. Castro[b], V. Madrazo[a], D. Andrés[a]

[a] Universidad de Cantabria, Ground and Materials Science and Engineering Department, LADICIM, Av/ Los Castros s/n, 39005, Santander, Cantabria, Spain, ciceros@unican.es

[b] Universidad de Cantabria, Ground and Materials Science and Engineering Department, Group of Geotechnical Engineering, Av/ Los Castros s/n, 39005, Santander, Cantabria, Spain,

ABSTRACT

This paper presents the analysis of the notch effect on granite and limestone fracture specimens. The research is based on the results obtained in an experimental programme composed of 84 fracture specimens, combining the two materials and 7 different notch radii varying from 0.15 mm up to 10 mm. The notch effect is analysed through the evolution of the apparent fracture toughness and the application of the Theory of the Critical Distances.

The results reveal a significant notch effect in the limestone, whereas the notch effect in the granite is negligible for the range of notch radii analysed. Both observations are justified by the corresponding critical distance of the material.

Keywords: Granite, limestone, notch effect, apparent fracture toughness, Theory of Critical Distances

1. Introduction

On many occasions, the load-bearing capacity of a structural component is conditioned by the existence of stress risers. These may have very different natures: cracks, notches, holes, welded joints, corners, etc, all of them having different approaches when the corresponding structural integrity is analysed. Rocks, whether they are naturally in the crust or whether they are industrially exploited (e.g., quarries, masonry) or operated (e.g., slopes, foundations, boreholes), have to sustain loads, and the presence of stress risers may play a key role in the corresponding structural integrity.

This paperfocuses on the fracture analysis of rocks containing notch-type defects and subjected to tensile stresses. Rock fracture mechanics (e.g., Aliabadi, 1999; Jeager et al., 2007 Whittaker et al., 1992) conveniently addresses those situations where it may be assumed that the analysed stress riser behaves as a crack-type defect, such as different applications of rock cutting, hydraulic fracturing or underground excavation. However, notch-type defects generate less demanding stress fields than crack-like defects, so it may be overly conservative to proceed on the assumption that notches behave like sharp cracks, coupled with the use of ordinary fracture mechanics. Numerous papers may be found in the literature providing different models of the stress field in the notch tip (e.g., Creager and Paris, 1967; Glinka and Newport, 1987; Pluvinage, 1998; Timoshenko and Goodier, 1951; Weiss, 1962). Basically, they all suggest a reduction in the stress acting perpendicular to the notch plane, in such a way that the larger the notch radius the more significant the stress reduction. This generally has direct consequences on the resistant behaviour of structural components (e.g., Cicero et al., 2012; Madrazo et al., 2012; Neuber, 1958; Peterson, 1958; Pluvinage, 1998; Taylor, 2007). Thus, in most cases, a given component has a higher load-bearing capacity and apparent fracture toughness in notched conditions than in cracked conditions. However, sometimes sharp notches behave like cracks and also blunt notches may not penalise the load-bearing capacity (beyond the corresponding

reduction in the resistant section). Additionally, the terms "sharp" and "blunt" are not absolute, but rather they depend on the material: there are materials that present a clear notch effect (e.g., increase in load-bearing capacity and apparent fracture toughness) for very small notch radii (e.g, Madrazo et al., 2012), and there are others that require a certain notch radius to develop a notch effect (e.g., Cicero et al., 2012). This particular nature of notches has led to a great deal of research work over the last few decades, aiming to provide specific tools for the assessment of notched components, beyond the simple and generally overconservative application of ordinary fracture mechanics. However, the analysis of these phenomena in rocks has been scarce, as detailed in the following section.

Moreover, size effects are an important issue in rock fracture mechanics, given that the material behaviour (e.g., fracture toughness, tensile strength) and the notch sensitivity may change with the size of the component being analysed (Bazant (1984), Bazant (1997), Bazant (2000), Borodich (1999), Carpinteri (1982), Carpinteri (1984), Dyskin (1997), Gjorv et al. (1977), Shah (1990)). Here, it should be noted that size effects are not directly addressed in this work, so that the obtained material parameters may not be transferable to different scales (e.g., massive rocks).

With all this, Section 2 of this paper presents the Theory of Critical Distances (TCD) as a tool for the assessment of notch-type defects in rocks, Section 3 gathers the description of the materials and the experimental programme, Section 4 provides the results and the corresponding discussion and, finally, Section 5 presents the conclusions.

2. Theoretical background: analysis of notches and the Theory of Critical Distances.

The stress distribution at the region ahead of a notch tip may be represented in a bi-logarithmic plot, as shown in Figure 1, where three regions can be distinguished (Niu et al., 1994;

Pluvinage, 1998). Region I corresponds to a nearly constant stress zone, region II is a transition zone, and region III is a zone where stresses follow the expression:

$$\sigma_{yy} = \frac{K_\rho}{(2\pi r)^\alpha} \quad (1)$$

where K_ρ is the notch stress intensity factor and α is a material constant for a given notch radius.

There are two main failure criteria in notch theory: the global fracture criterion and local fracture criteria (Bao and Jin, 1993; Pluvinage, 1998). The global criterion establishes that failure occurs when the notch stress intensity factor reaches a critical value, K_ρ^c, which depends on the notch radius and the material:

$$K_\rho = K_\rho^c \quad (2)$$

K_ρ defines the stress and strain fields in the vicinity of the notch tip, as shown in equation (1). This approach is analogous to that proposed by linear-elastic fracture mechanics for the analysis of cracks, but its application is very limited because of the lack of analytical solutions for K_ρ (in contrast with the case of K_I, e.g., API579-1/ASME FFS-1, 2007; BS7910, 2005; FITNET FFS Procedure, 2008; R6, 2001) or/and standardised procedures for the experimental definition of K_ρ^c (in contrast with the case of K_{IC}, e.g., ASTM E 1820-09e1, 2009).

Concerning local criteria, these are based on the stress-strain field on the notch tip and have more applicability than global criteria from a practical point of view. Among them, those criteria belonging to the TCD stand out. The Theory of Critical Distances (TCD) is essentially a group of methodologies, all of which use a characteristic material length parameter (the critical distance, *L*) when performing fracture assessments (Taylor, 2007; Taylor et al., 2004). The origins of the TCD date back to the middle of the twentieth century, with the works of Neuber (1958) and Peterson (1959), but it has been in the last years, driven by the proliferation of finite element stress analyses, that this theory has been scientifically analysed and applied to different types of materials (metals, ceramics, polymers and composites), failure or damage processes

(basically fracture and fatigue) and conditions (e.g., linear-elastic vs. elastoplastic) (e.g., Cicero et al., 2012; Cicero et al., 2013; Madrazo et al., 2012; Susmel and Taylor, 2003; Susmel and Taylor, 2010; Taylor, 2001; Taylor, 2007; Taylor and Wang, 2000; Taylor et al, 2004).

The above-mentioned critical distance is usually referred to as L and its expression is:

$$L = \frac{1}{\pi}\left(\frac{K_{IC}}{\sigma_0}\right)^2 \tag{3}$$

where K_{IC} is the material fracture toughness and σ_0 is a characteristic material strength parameter named the inherent strength, usually larger than the ultimate tensile strength (σ_u), which requires calibration. Only in those situations where there is a linear-elastic behaviour at both the micro and the macroscale (e.g., fracture of rocks) does σ_0 coincide with σ_u.

Among the different methodologies included within the TCD, two of them are particularly simple to apply: the Point Method (PM), also known as the Stress Method, and the Line Method (LM). Both of these are based on the stress field at the defect tip. Other methodologies, such as Finite Fracture Mechanics (FFM) and the Imaginary Crack Method are based on the stress intensity factor and their application is not so straightforward. In any case, as stated by Taylor (2007), the predictions made by all these methodologies are very similar, so that only the PM and the LM, those with a far simpler application, will be considered here.

The Point Method (PM) is the simplest methodology, and it assumes that fracture occurs when the stress reaches the inherent strength (σ_0) at a certain distance from the defect tip, r_c. It considers that the material has linear-elastic behaviour, and from the stress field in a crack tip at failure (Anderson, 2004; Taylor, 2007) and the definition of L (equation (3)), it is straightforward to demonstrate that r_c is L/2:

$$\frac{K_{IC}}{\sqrt{2\pi r_c}} = \sigma_0 \Rightarrow r_c = \frac{1}{2\pi}\left(\frac{K_{IC}}{\sigma_0}\right)^2 = \frac{L}{2} \tag{4}$$

The PM failure criterion is, therefore:

$$\sigma\left(\frac{L}{2}\right)=\sigma_0 \tag{5}$$

On the other hand, the Line Method (LM) assumes that fracture occurs when the average stress along a certain distance, d (starting from the defect tip), reaches the inherent strength, σ_0. Again, from the stress field in a crack tip at failure and the definition of L, it is easy to demonstrate that d is equal to 2L:

$$\frac{1}{d}\int_0^d \frac{K_{IC}}{\sqrt{2\pi r}}dr=\frac{2}{\sqrt{2\pi}}\frac{K_{IC}}{d^{1/2}}=\sigma_0 \Rightarrow d=\frac{4}{2\pi}\left(\frac{K_{IC}}{\sigma_0}\right)^2=2L \tag{6}$$

Therefore, the LM failure criterion is:

$$\frac{1}{2L}\int_0^{2L}\sigma(r)dr=\sigma_0 \tag{7}$$

The TCD, and then the PM and the LM, allows the fracture assessment of components with any kind of stress riser to be performed. As an example, when using the PM it would be sufficient to perform two fracture tests on two specimens with different types of defects (e.g., sharp notch and blunt notch). The corresponding stress-distance curves at fracture, which can be determined by using analytical solutions or finite element methods, cross each other at a point with coordinates ($L/2,\sigma_0$), as shown in Figure 2. The prediction of the fracture load of any other component made of the same material and containing any other kind of defect would require the definition of the corresponding stress field, the fracture load being that one for which equation (5) is fulfilled.

In the case of rocks, with linear-elastic behaviour at both the micro and the macro scales, the application of the TCD is even simpler, given that there is no need to calibrate σ_0 (it coincides with σ_u) and L (directly provided by equation (3) once both K_{IC} and σ_u are known). Despite such simplicity and the enormous potential of the TCD for the analysis of fracture processes, as it has been demonstrated for a wide variety of materials, the application of this theory in rocks has

been very limited. To the knowledge of the authors, Lajtai (1972) was the first author applying the PM on rocks, being followed by Ito and Hayashi (1991) and Ito (2008), who successfully applied the PM for the analysis of hydraulic fracturing in a wellbore. Such works have been cited by other authors (e.g., Bunger et al., 2010; Shimizu et al., 2011), but the application of the TCD in rocks has not been further developed.

To finish with this overview of the TCD, it should be noted that this theory allows components containing U-shaped notches to be analysed relatively simply: the PM and the LM provide expressions (whose justification, based on the Creager and Paris (1968) notch tip stress distribution, may be found in Taylor (2007)) for the apparent fracture toughness (K_{IN}) exhibited by this type of notched components. This parameter reduces the fracture analysis in a component having a U-shaped notch to an equivalent situation in a cracked component, with the only particularity of considering K_{IN} instead of K_{IC}. Thus, fracture occurs when:

$$K_I = K_{IN} \tag{8}$$

K_I is the stress intensity factor for a crack with the same extension of the notch, and K_{IN} may be obtained using the following expressions (ρ being the notch radius):

$$K_{IN} = K_{IC} \frac{\left(1+\frac{\rho}{L}\right)^{3/2}}{\left(1+\frac{2\rho}{L}\right)} \tag{9}$$

when using the PM , and

$$K_{IN} = K_{IC} \sqrt{1+\frac{\rho}{4L}} \tag{10}$$

when using the LM. Equations (9) and (10) are valid for long narrow notches, given that the application of the Creager-Paris stress distribution is limited to such geometric conditions.

3. Materials and experimental programme

3.1. Materials

The analysis of the notch effect in rocks is particularised here to two representative hard brittle rocks: biotite granite and oolitic limestone. The geological location of these rocks is the centre and the south-east of Spain, respectively. Table 1 present some of their nominal technical properties (obtained following UNE-EN 12407, 2007; UNE-EN 13755, 2008; UNE-EN 14157, 2005; UNE-EN 14231, 2004; UNE-EN 1936, 2007), while figures 3 and 4 show the corresponding microstructures observed with optical and scanning electron microscopy (SEM). These two rocks are used for industrial applications and, consequently, they are highly homogeneous (at the macro-scale), isotropic, non-weathered rocks.

3.2. Compression tests and splitting tensile strength tests

Six compression tests were performed on each material following UNE-EN 1936 (2007) and UNE-EN 14580 (2006). Analogously, six splitting tensile tests (Brazilian test) were performed on both the granite and the limestone following UNE 22950-2 (1990). Here, it should be noted that the tensile strength is a key parameter for the application of the TCD (see equation (3), where σ_0 coincides with σ_u).

3.3. Fracture toughness tests

As shown and summarised by Amaral et al. (2008), there are several methodologies for the assessment of fracture toughness in rocks (e.g., ASTM-PS70, 1997; CEN/TS 14425-1, 2003; Fowel and Xu, 1994; Hashida and Takahashi, 1993; Lim et al., 1994; Ouchterlony, 1988). Here the CEN/TS 14425-1 (2003) methodology has been selected to determine this material property. The methodology, which was originally proposed by Srawley and Gross (1976) for ceramic

materials, uses SENB specimens tested in 4-point bending conditions, whose geometry is shown in Figure 5. A straight notch was cut using diamond-wire saw equipment with a wire of 0.3 mm diameter (notch radius, ρ= 0.15 mm). The tests, six for each material, were performed in displacement control, the loading rate being 0.05 mm/min. In all the tests, both the applied load and the vertical displacement were recorded, so that the fracture (failure) load (F) could be easily determined. The material fracture toughness (K_{IC}) is then obtained through the following formulation (CEN/TS 14425-1, 2003; Srawley and Gross, 1976):

$$K_{IC} = \frac{F \cdot Y}{b \cdot h^{1/2}} \tag{11}$$

where b is the specimen thickness, h is the specimen height and Y is the compliance factor given by:

$$Y = \frac{3 \cdot (L_o - L_i) \cdot \alpha_0^{1/2} \cdot X}{2h \cdot (1-\alpha_0)^{3/2}} \tag{12}$$

with

$$X = 1.9887 - \left[\frac{\left(3.49 - 0.68\alpha_0 - 1.35\alpha_0^2\right) \cdot \alpha_0 \cdot (1-\alpha_0)}{(1+\alpha_0)^2} \right] - 1.32\alpha_0 \tag{13}$$

L_o and L_i being the spans between the outer and inner loading points, respectively, and $\alpha_0 = a_0/h$. In this case L_o=120mm, L_i=60 mm. a_0 (the notch length) was measured through an optical microscope at 50x magnification and varies between 7 mm and 8 mm ($0.35 \leq \alpha_0 \leq 0.40$).

The experimental setup is shown in Figure 6.

3.4. Apparent fracture toughness tests

The experimental procedure explained above was applied to fracture specimens with notch radii of 0.5 mm, 1 mm, 2 mm, 4 mm, 7 mm and 10 mm (see Figure 5), in order to obtain the corresponding apparent fracture toughness (K_{IN}), which is that one obtained by the application of the cracked specimen formulation to notched specimens. Here, it should be noted that fracture toughness testing methodologies for rocks accept a limited finite radius on the notch tip (e.g., 0.15 mm), assuming a similar behaviour to that obtained in cracked conditions and considering that the introduction of a proper crack with controlled geometry is not feasible. Thus, the results of fracture toughness tests are actually apparent fracture toughness values on which the notch effect is considered to be negligible.

With all this, six specimens per material and notch radius were tested, obtaining the corresponding fracture load. Then, equations (11) to (13) were applied, providing the apparent fracture toughness.

4. Results and discussion

The mechanical properties obtained in compression and splitting tensile strength tests are shown in Table 2, where E_{50} represents the tangent elastic modulus at 50% of fracture load. As an example, Figure 7 presents two examples of experimental curves obtained in the compression tests. The results are consistent with the literature (e.g., Kulhawy, 1975; Stagg and Zienkiewicz, 1969).

Tables 3 and 4 gather the results of fracture toughness tests (specimens with 0.15 mm notch radius) and apparent fracture toughness tests (specimens with notch radii from 0.5 mm up to 10 mm), respectively. Here it should be noted that, in all tests, fracture took place across the

middle plane of the specimens, starting from the notch tip. The fracture surfaces were basically flat and had a brittle aspect.

Figure 8 shows, as an example, the obtained load-displacement curves of the fracture toughness tests, where it can be observed how the granite develops higher values of load-bearing capacity, also leading to higher values of fracture toughness. Analogously, Figure 9 shows the load-displacement curves obtained in the apparent fracture toughness tests performed on specimens with 10 mm notch radii. In the case of the granite (Figure 9a), it can be observed that the load-bearing capacity is rather similar in terms of average values to that obtained in fracture toughness tests (see Figure 8a); in the case of the limestone (Figure 9b) there is a noticeable increase in the loadbearing capacity when compared to the results obtained in fracture toughness tests (Figure 8b).

The resulting average fracture toughness values are 1.24 $MPam^{1/2}$ for the granite and 0.72 $MPam^{1/2}$ for the limestone. These values, together with the corresponding tensile strength values (see Table 2), allow the critical distance (L) of the materials to be obtained using equation (3) and assuming that σ_0 is equal to σ_u. Thus, L gives 6.04 mm in the granite and 2.71 mm in the limestone, that is, 6.0 and 3.4 times the corresponding grain size. This is in agreement with the relation provided by Usami et al. (1986) for ceramic materials, in which L ranges between one and ten times the grain size, or the values obtained by Ito and Hayashi (1991) for Kofu andesite (L=6.8 mm) and Honkomatsu andesite (L=3.2 mm). As mentioned below, this may have a physical meaning in the fracture process.

The comparison between L and the notch geometry may provide interesting observations, as explained by Taylor (2012):

- Comparing L to notch length (a): when the normalised notch length is much lower than the unity ($a/L << 1$) then the notch is harmless and it does not reduce the strength of the

body. Here the notch length varies between 7 mm and 8 mm, so the above mentioned condition is not fulfilled. In any case, as stated in Taylor (2012) this dimensionless number can be defined more generally as the normalised defect size (for any kind of defect, not just a notch), and as long as this number is sufficiently lower than one, the corresponding defect is harmless. As an example, an internal spherical pore with a 1 mm radius would be harmless in the granite.

- Comparing L to notch radius (ρ): when the normalised notch radius is lower than 1 (ρ/L < 1) the corresponding notch behaves as a crack of the same length (Taylor, 2012). If ρ/L is much higher than one (ρ/L >> 1) the corresponding notch may be simply analysed through the elastic stress concentration factor (K_t). Therefore, in the case of granite and for the size of components considered here, those notches whose notch radius is smaller than 6.04 mm would behave as cracks, whereas in the case of the limestone this crack behaviour would be observed for notch radii smaller than 2.71 mm. This is an important observation for geological materials: given that the values of the critical distance are relatively high in this type of materials (in the order of mm, see also Dempsey et al. (1999), and Ito and Hayasi (1991)), notches with significant root radii may behave as cracks and could be analysed by using ordinary fracture mechanics (i.e., not considering any notch effect).

Another consequence of the high values obtained for the critical distance is the adequacy of using notched specimens (instead of cracked) to the experimental determination of the fracture toughness (K_{IC}) in rocks: as long as the notch radius is smaller than the critical distance of the material being analysed (generally in the order of several mm), the obtained apparent fracture toughness (K_{IN}) is equal to the material fracture toughness.

Figure 10 presents the apparent fracture toughness results:

- In the case of the granite results, it can be observed that the notch effect is basically negligible for the range of notch radii considered in the analysis (up to 10 mm). This basically agrees with the above comments concerning the normalised notch radius: given that L is 6.04 mm, the expected notch effect for notch radii below this value (0.5 mm, 1 mm, 2 mm and 4 mm) is null, whereas some notch effect should be observed for higher notch radii (7 mm and 10 mm). Thus, the results corresponding to a 7 mm notch radius do present a slight notch effect (apparent fracture toughness higher than the fracture toughness obtained in 0.15 mm notch radius specimens). However, the results obtained in specimens with a 10 mm notch radius do not present any notch effect and their average value is very similar to that obtained with much lower radii. There is no physical explanation for this lack of notch effect, and here it has been attributed to the obtained experimental scatter (i.e., a higher number of tests would show the existence of notch effect).

  The figure also shows the predictions provided by the LM (for the sake of simplicity, the predictions provided by the PM are not included) when applying equation (10). It should be noted that blunter notches are beyond the theoretical application range of the apparent fracture toughness predictions provided by the TCD. The solid line represents the predictions obtained when the value of L provided by equation (3) is considered, whereas the dotted line represents the best fit of equation (10) providing least squares. The fitting process has been performed in a region dominated by negligible notch effect, so the obtained value of L (46.6 mm) has no physical meaning, and cannot be compared to that obtained through equation (3).

- In the case of the limestone, its lower value of L allows the notch effect to be much clearer within the range of notch radii considered in this work. Those radii above 2.71 mm (4 mm, 7 mm and 10 mm) should present notch effect, whereas the other radii (0.5

mm, 1 mm and 2 mm) should provide similar apparent fracture toughness values to those obtained in the fracture toughness tests. Considering average values, the experimental results confirm these predictions.

In this case the LM provides reasonably good predictions of the apparent fracture toughness, regardless of the critical distance considered: that given by equation (3) (solid line) or the one given by the best fit providing least squares (L= 3.4 mm, dotted line). The two obtained values of L present certain difference, but it should be noted that the consequences of such difference is rather limited, given that L is squared in equation (10). Also, the predictions provided by the TCD are reasonable even for blunter notches, even though they are beyond the application range of equation (10).

Hence, the critical distance of these two materials (and the ratio ρ/L) reasonably explains why, for the notch radii considered here, the notch effect has been found to be negligible in the granite and significant in the limestone. This may be physically related with the corresponding material microstructure: Taylor (2007) presents a summary of works that have analysed the physical meaning of the critical distance. The first comment on this is that, depending on the material being analysed, L may take values that range from the atomic separation (Pugno and Ruoff, 2004) up to meters (Dempsey et al, 1999), for certain specific situations such as nanomaterials and sea ice, respectively, with typical values from tens of microns up to a number of centimetres. Taylor (2007) distinguishes here two situations when trying to relate the critical distance to the material characteristics: in materials such as ceramics and steels the critical distance is simply related to the microstructure, especially to the grain size (d), which acts as a barrier to crack propagation and thus plays a key role in the crack growth; in other materials such as composites and certain polymers L is associated to a damage zone. Here, the average grain size of the granite is significantly larger (25%) than the average grain size of limestone (see Table 1). Moreover, the grains in the granite have less uniform sizes (see figures 3 and 4),

so this material presents much higher maximum grain sizes than the limestone. These larger grains may facilitate the fracture process even when the notch radius is significant.

Finally, as mentioned in the introduction, the transferability of the results obtained here to other scales is not straightforward, and it is not addressed in this work. Size effects have basically two components: a geometric component (stress gradients may vary with the scale) and a statistical component associated to the increasing possibility of large defects in larger volumes of material. The TCD implicitly includes the geometric component but it does not consider any statistical effect. Moreover, the fracture toughness and the ultimate tensile strength may vary with the size of the component, so L may also have a scaling effect.

5. Conclusions

This paper presents the analysis of the notch effect on biotite granite and oolitic limestone. The analysis is based on two main questions: firstly, the results obtained in an experimental programme composed of 84 SENB specimens tested in 4-point bending conditions, covering notch radii from 0.15 mm (which are assumed to have crack-like behaviour) up to 10 mm. The programme also includes compression and splitting tensile strength tests. Secondly, the Theory of Critical Distances (Line Method approach) is applied to the fracture tests. The main conclusions, for the component sizes considered here, are the following:

- The critical distance (L) gives 6.04 mm for the granite and 2.71 mm for the limestone. These values allow the load-bearing capacity of any structural element made of these materials to be predicted by applying the TCD approaches (e.g., the PM or the LM).
- Those defects whose size is much smaller than L are harmless (e.g., in granite, a pore with a 1 mm radius)
- Those notches whose radius is smaller than L behave as cracks. This means, for example, that granite specimens containing notches with a 4 mm notch radius provide

the same fracture resistance (apparent fracture toughness) as that obtained with a lower radius (including crack-type defects).

- This supports the hypothesis of the different fracture toughness testing procedures, consisting in the assumption of a similar behaviour between crack-type defects and notch-type defects, as long as the notch radius is sufficiently limited.
- Finally, the TCD justifies the negligible (or very limited) notch effect observed in the granite, as well as the significant notch effect observed in the limestone. In both cases the predictions provided by the TCD (through the LM) are reasonable when compared to the experimental results. However, a more sound validation of the application of the TCD in rocks would require additional testing in other types of rocks, as well as a wider range of notch geometries (e.g., larger notch radii and notch depths).

Acknowledgments

The authors of this work would like to express their gratitude to the Spanish Ministry of Science and Innovation for the financial support of the project MAT2010-15721: ‘‘Análisis de integridad estructural en defectos tipo entalla’’ (Structural integrity assessments of notch-type defects), on the results of which this paper is based.

References

Aliabadi, M.H., 1999. Fracture of rock. WIT Press.

Amaral, P.M., Guerra Rosa, L., Cruz Fernandes, J., 2008. Assessment of fracture toughness in ornamental stones. Int. J. Rock. Mech. Min. Sci. 45, 554-563.

Anderson, T.L., 2004. Fracture mechanics: fundamentals and applications, Third ed. CRC Press. Florida.

API 579-1/ASME FFS-1 Fitness-For-Service, 2007. American Society of Mechanical Engineers, New York.

ASTM E 1820-09e1, 2009. Standard test method for measurement of fracture toughness. American Society for Testing and Materials, Philadelphia.

ASTM-PS70:1997, 1997. Provisional test methods for determination of fracture toughness of advanced ceramics at ambient temperatures. American Society for Testing and Materials, Philadelphia.

Bao, Y., Jin, Z., 1993. Size effects and mean strength criterion for ceramics. Fatig. Fract. Eng. Mater. Struct. 16, 829-835.

Bazant, Z. P., 1984. Size effect in blunt fracture: concrete, rock, metal. J. Eng. Mech. 110, 518-535.

Bazant, Z. P., 1997. Scaling of quasibrittle fracture: asymptotic analysis. Int. J. Fract. 83, 19-40.Bazant, Z. P., 2000. Size effect. Int. J. Solids Struct. 37, 69-80.

BS 7910: 2005, 2005. Guide to methods for assessing the acceptability of flaws in metallic structures. British Standards Institution, London.

Borodich, F. M., 1999. Fractals and fractal scaling in fracture mechanics. Int. J. Fract. 95, 239-259.

Bunger, A.P., Lakirouhani, A., Detournay, E., 2010. Modelling the effect of injection system compressibility and viscous fluid flow on hydraulic fracture breakdown pressure. In: Rock Stress and Earthquakes-Proceedings of the 5th International Symposium on In-Situ Rock Stress, 59-67.

Carpinteri, A., 1982. Notch sensitivity in fracture testing of aggregative materials. Eng. Fract. Mechanics. 16, 467-481.

Carpinteri, A., 1994. Fractal nature of material microstructure and size effects on apparent mechanical properties. Mech. Mater. 18, 89-101.

CEN/TS 14425-1:2003, 2003. Advanced technical ceramics—test methods for determination of fracture toughness of monolithic ceramics—part 1: guide to test method selection. European Committee for Standarization.

Cicero, S., Madrazo, V., Carrascal, I.A., 2012. Analysis of notch effect in PMMA by using the Theory of Critical Distances. Eng. Fract. Mech. 86, 56-72.

Cicero, S., Madrazo, V., García, T., Cuervo, J., Ruiz, E., 2013. On the notch effect in load bearing capacity, apparent fracture toughness and fracture mechanisms of polymer PMMA, aluminium alloy Al7075-T651 and structural steels S275JR and S355J2. Eng. Fail. Anal. 29, 108-121.

Creager, M., Paris, C., 1967. Elastic field equations for blunt cracks with reference to stress corrosion cracking. Int. J. Fract. 3, 247-252.

Dempsey, J.P., Adamson, R.M., Mulmule, S.V., 1999. Scale effect on the in-situ tensile strength and failure of ice. Part II: first-year sea ice at Resolute, NWR. Int. J. Fract. 95, 347-366.

FITNET Fitness-for-Service (FFS) Proceure - Volume 1, 2008. GKSS, Geesthacht.

Dyskin, A. V., 1997. Crack growth criteria incorporating non-singular stresses: size effect in apparent fracture toughness. Int. J. Fract. 83, 191-206.

Fowell, R.J., Xu, C., 1993. The cracked chevron-notched Brazilian disc test—geometrical considerations for practical rock fracture-toughness measurement. Int. J. Rock. Mech. Min. Sci. Geomech. Abstr. 30, 821-824.

Gjorv, O. E., Sorensen, S. I., Arnesen, A., 1977. Notch sensitivity and fracture toughness of concrete. Cement Concr. Res. 7, 333-344.

Glinka, G., Newport, A., 1987. Universal features of elastic notch tip stress fields. Int. J. Fatigue. 9, 143-150.

Hashida, T., Takahashi, H., 1993. Significance of AE crack monitoring in fracture-toughness evaluation and nonlinear rock fracture-mechanics. Int. J. Rock Mech. Min. Sci. Geomech. Abstr. 30, 47-60.

Ito, T., 2008. Effect of pore pressure gradient on fracture initiation in fluid saturated porous media: Rock. Eng. Fract. Mech. 75, 1753-1762.

Ito, T., Hayasi, K., 1991. Physical background to the breakdown pressure in hydraulic fracturing tectonic stress measurements. Int. J. Rock Mech. Min. Sci. Geomech. Abstr. 28, 285-293.

Jeager, J.C., Cook, N.G., Zimmerman, R., 2007. Fundamentals of Rock Mechanics, 4th edition. Wiley-Blackwell.

Kulhawy, F.H., 1975. Stress deformation properties of rock and rock discontinuities. Eng. Geol. 9, 327-350.

Lataji, E.Z, 1972. Effect of tensile stress gradient on brittle fracture initiation. Int. J. Rock Mech. Min. Sci. Geomech. Abstr. 9, 569-578

Lim, I.L, Johnston, I.W., Choi, S.K., 1994. Assessment of mixed-node fracture toughness testing methods for rock. Int. J. Rock Mech. Min. Sci. Geomech. Abstr. 31, 265-272.

Madrazo, V., Cicero, S., Carrascal, I.A., 2012. On the point method and the line method notch effect predictions in Al7075-T651. Eng. Fract. Mech. 79, 363-379.

Neuber, H., 1958. Theory of notch stresses: principles for exact calculation of strength with reference to structural form and material. Springer Verlag, Berlin.

Niu, L.S, Chehimi, C., Pluvinage, G., 1994. Stress Field Near a Large Blunted V Notch and Application of the Concept of Critical Notch Stress Intensity Factor to the Fracture of Very Brittle Materials. Eng. Fract. Mech. 49, 325-335.

Ouchterlony, F., 1988. ISRM suggested methods for determining the fracture-toughness of rock. Int. J. Rock Mech. Min. Sci. Geomech. Abstr. 25, 71-96.

Peterson, R.E., 1959. Notch sensitivity, in: Sines, G., Waisman, J.L. (Eds.), Metal fatigue. McGraw Hill, New York, pp. 293–306.

Pluvinage, G., 1998. Fatigue and fracture emanating from notch; the use of the notch stress intensity factor. Nucl. Eng. Des. 185, 173-184.

Pugno, N., Ruoff, R., 2004. Quantized fracture mechanics. Philosophical Magazine. 84, 2829-2845.

R6, 2001. Assessment of the integrity of structures containing defects. British Energy Generation Limited, Revision 4.

Shah, S. P., 1990. Size-effect method for determining fracture energy and process zone size of concrete. Mat. Struct. 23, 461-465.

Shimizu, H., Murata, S., Ishida, T., 2011. The distinct element analysis for hydraulic fracturing in hard rock considering fluid viscosity and particle size distribution. Int. J. Rock. Mech. Min. Sci. 48, 712-727.

Srawley, J., Gross, B., 1976. Cracks and fracture. ASTM Spec. Tech. Publ. 601, 559-579.

Stagg, K.G., Zienkiewicz, O.C., 1969. Rock mechanics in engineering practice. Wiley.

Susmel, L., Taylor, D., 2003. Fatigue design in the presence of stress concentrations. Int. J. Strain Anal. Eng. Compon. 38, 443-452.

Susmel, L., Taylor, D., 2010. An elasto-plastic reformulation of the Theory of Critical Distances to estimate lifetime of notched components failing in the low/medium-cycle fatigue regime. J. of Eng. Mat. and Tech., Trans. of ASME. 132, 0210021-28.

Taylor, D., 2001. A mechanistic approach to critical-distance methods in notch fatigue. Fatigue Fract. Eng. Mater. Struct. 24, 215-224.

Taylor, D., 2007. The theory of critical distances: a new perspective in fracture mechanics. Elsevier.

Taylor, D., 2012. Applications of the theory of critical distances in failure analysis. Eng. Fail. Anal. 18, 543-549.

Taylor, D., Wang, G., 2000. The validation of some methods of notch fatigue analysis. Fatigue Fract. Eng. Mater. Struct. 23, 387-394.

Taylor, D., Merlo, M., Pegley, R., Cavatorta, M,P., 2004. The effect of stress concentrations on the fracture strength of polymethylmethacrylate. Mater. Sci. Eng. A382, 288-294.

Timoshenko, S., Goodier, J.N., 1951. Theory of Elasticity. McGraw-Hill.

UNE-EN 12407:2007, 2007. Métodos de ensayo para piedra natural. Estudio petrográfico. AENOR.

UNE-EN 13755:2008, 2008. Métodos de ensayo para piedra natural. Determinación de la absorción de agua a presión atmosférica. AENOR.

UNE-EN 14157:2005, 2005. Métodos de ensayo para piedra natural. Determinación de la resistencia a la abrasión. AENOR.

UNE-EN 14231:2004, 2004. Métodos de ensayo para piedra natural. Determinación de la resistencia al deslizamiento mediante el péndulo de fricción. AENOR.

UNE-EN 14580:2006, 2006. Métodos de ensayo para la piedra natural. Determinación módulo de elasticidad estático. AENOR.

UNE-EN 1926:2007, 2007. Métodos de ensayo para la piedra natural. Determinación de la resistencia a la compresión uniaxial. AENOR.

UNE-EN 1936:2007, 2007. Métodos de ensayo para piedra natural. Determinación de la densidad real y aparente y de la porosidad abierta y total. AENOR.

UNE 22950-2:1990, 1990. Propiedades mecánicas de las rocas. Ensayos para la determinación de la resistencia. Parte 2: resistencia a tracción. Determinación indirecta (ensayo brasileño). AENOR.

Usami, S., Kimoto, H., Takahashi, I., Shida, S., 1986. Strength of ceramic materials containing small flaws. Eng. Fract. Mech. 23, 745-761.

Weiss, V., 1962. Application of Weibull´s statistical theory of fracture to sheet specimens. Trans. ASME, paper No. 62-WA-270.

Whittaker, B.N., Singh, R.N., Sun G., 1992. Rock fracture mechanics: principles, design, and applications. Elsevier.

Figures

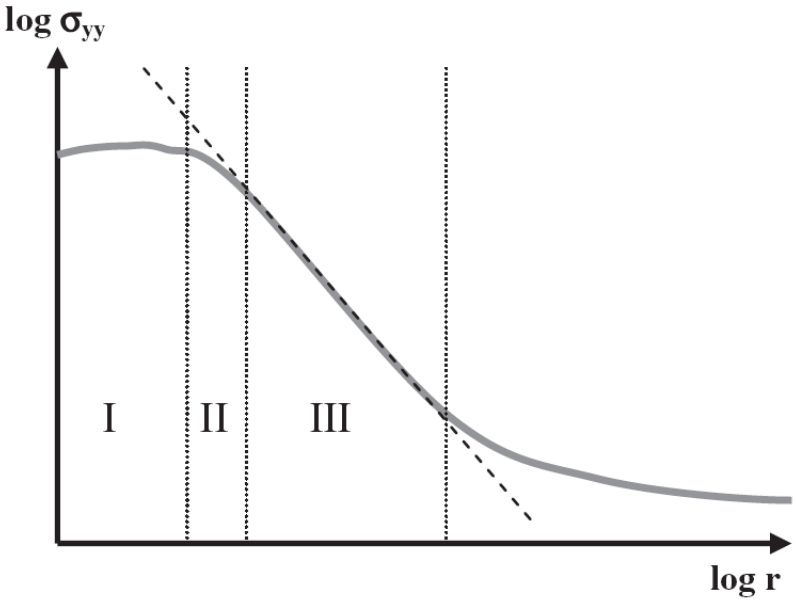

Figure 1. Schematic showing the stress distribution at a notch tip (bi-logarithmic).

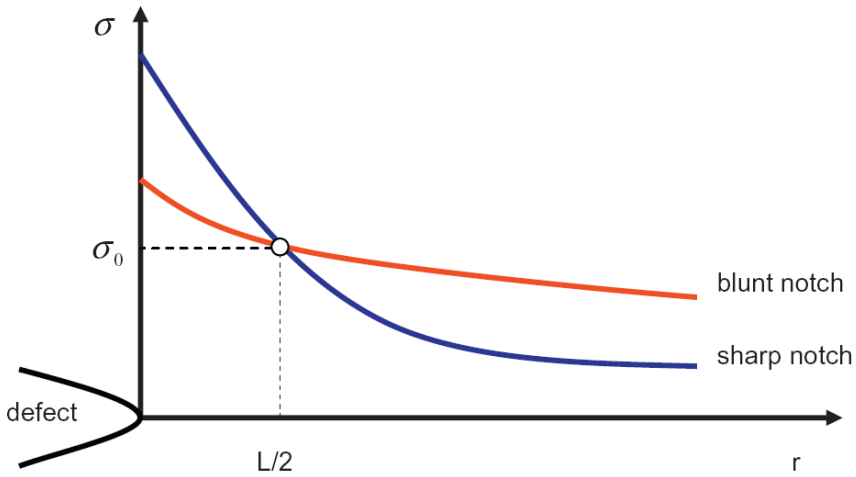

Figure 2. Obtaining L and σ_0 parameters.

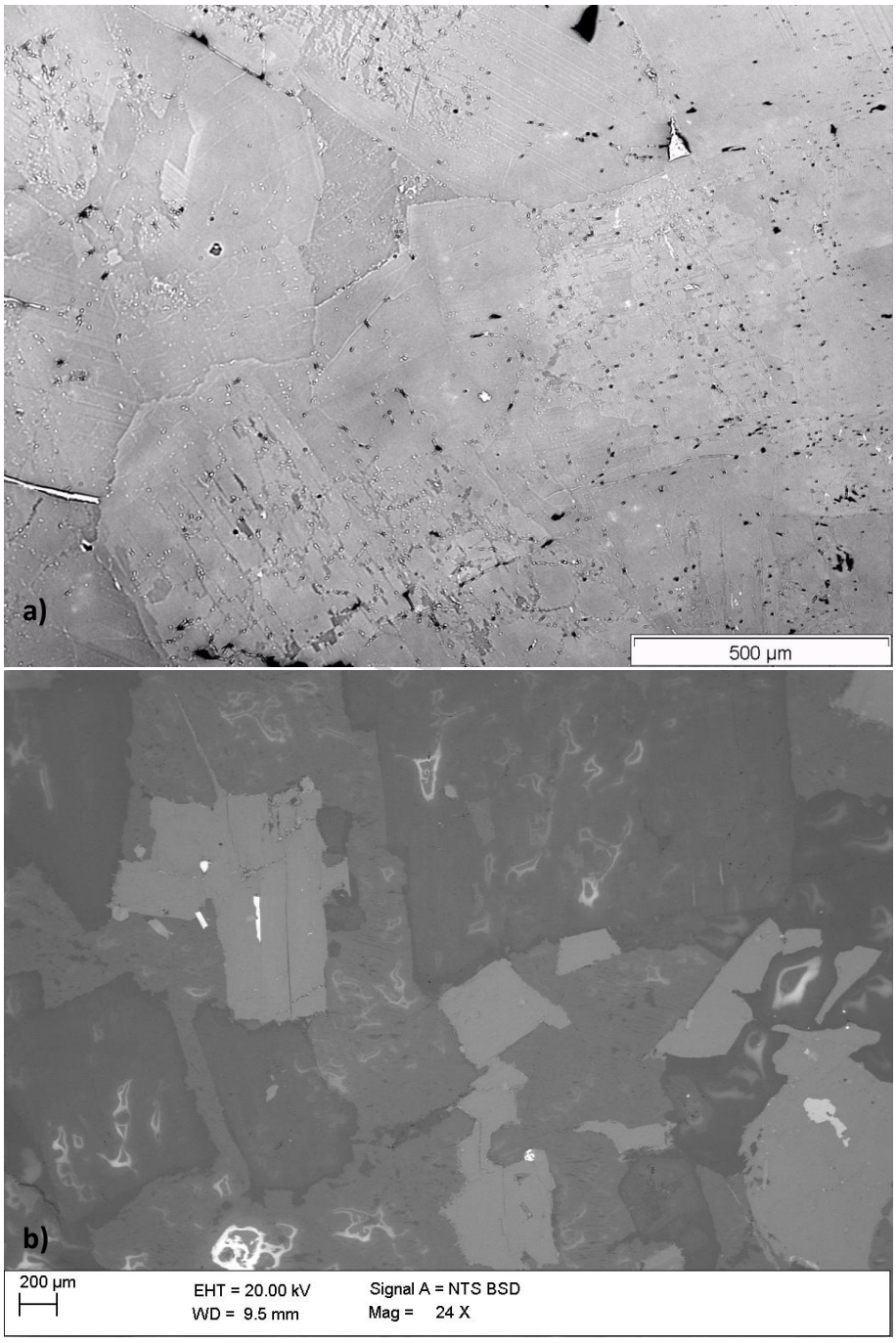

Figure 3. Microstructure of the granite being analysed: a) optical microscopy; b) SEM.

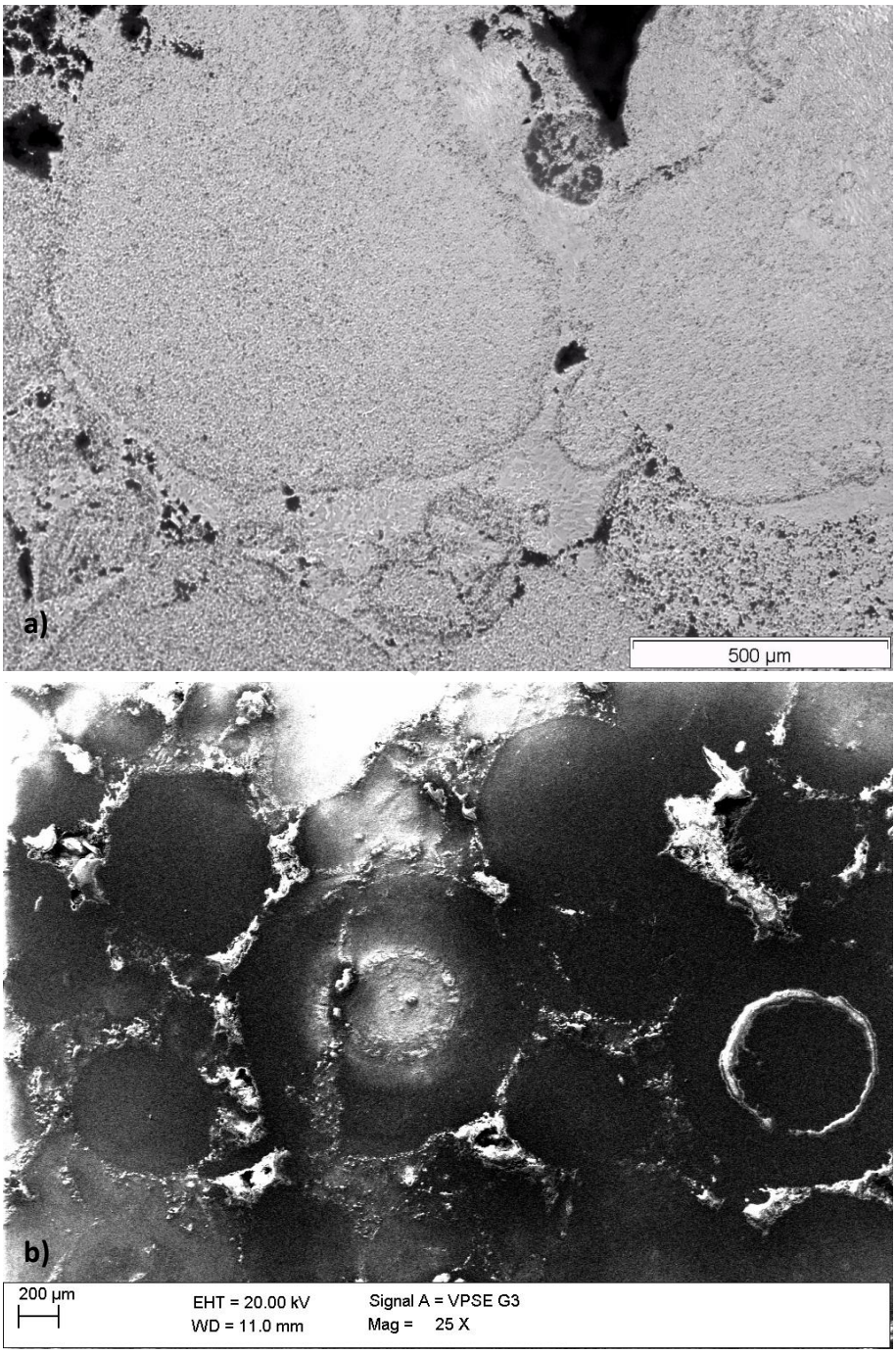

Figure 4. Microstructure of the oolitic limestone being analysed: a) optical microscopy; b) SEM.

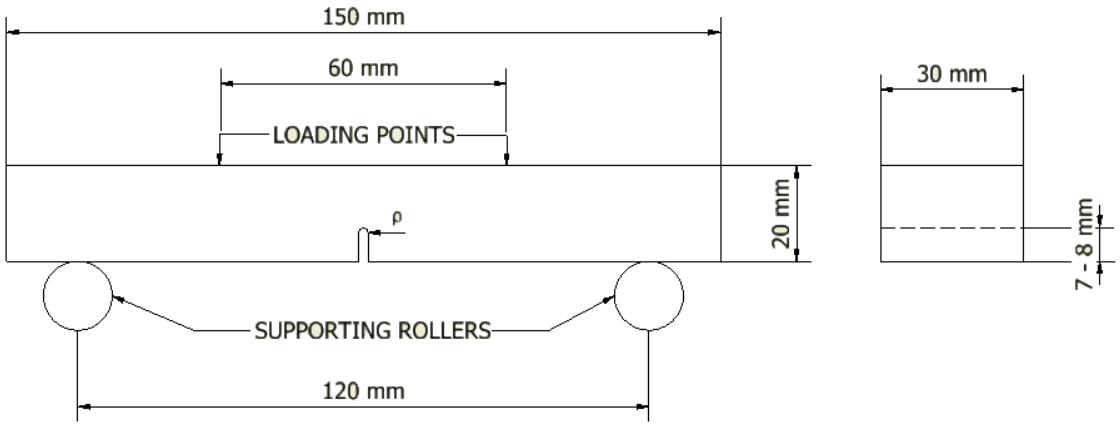

Figure 5. Schematic of fracture specimens. Dimensions in mm. Notch radii (ρ) varies from 0.15 mm (fracture toughness specimens) up to 10 mm.

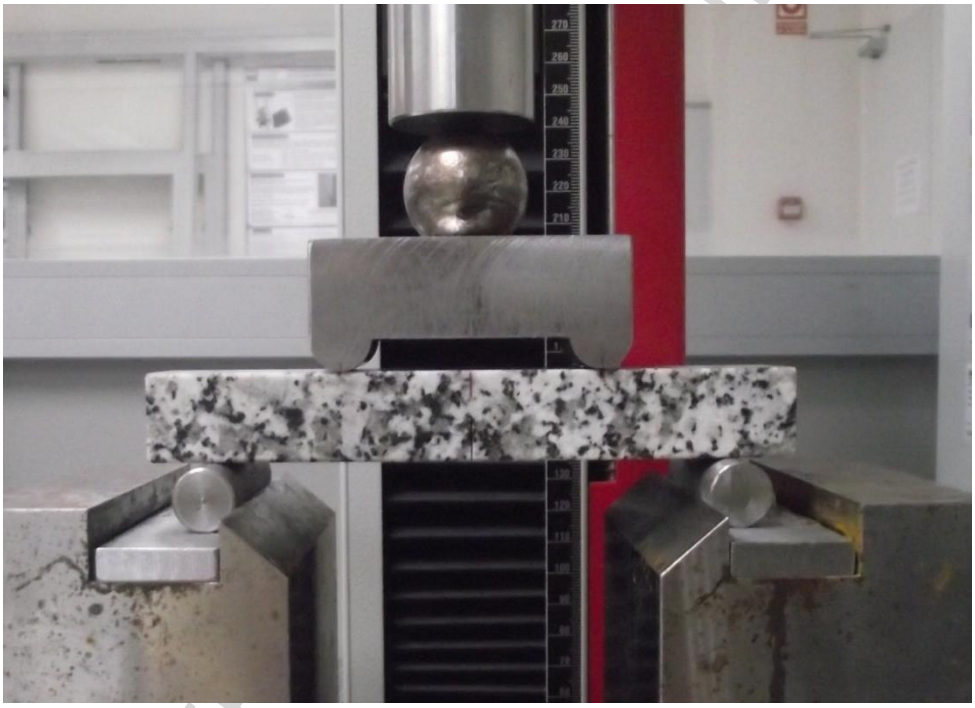

Figure 6. Experimental setup in fracture toughness tests.

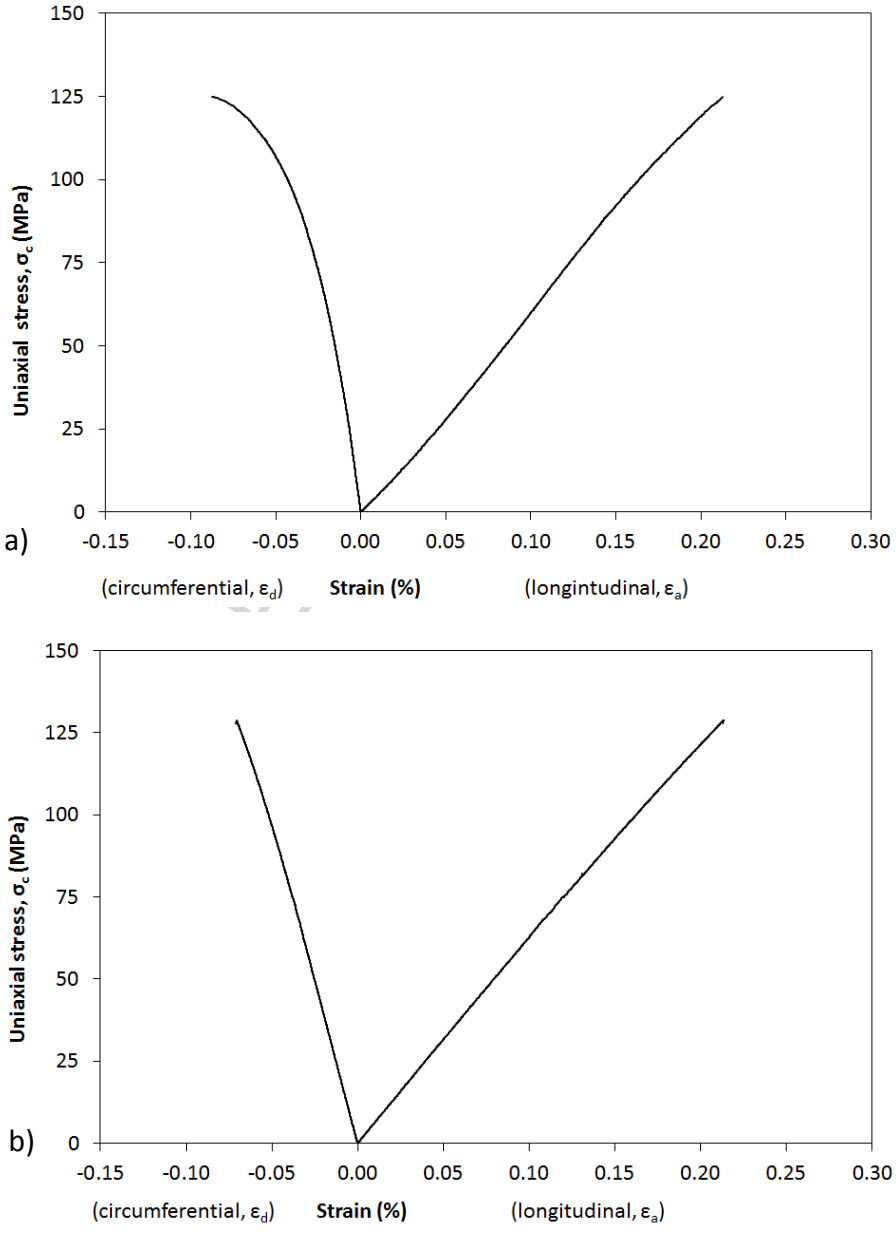

Figure 7. Stres-strain curves obtained in compression tests: a) granite; b) limestone.

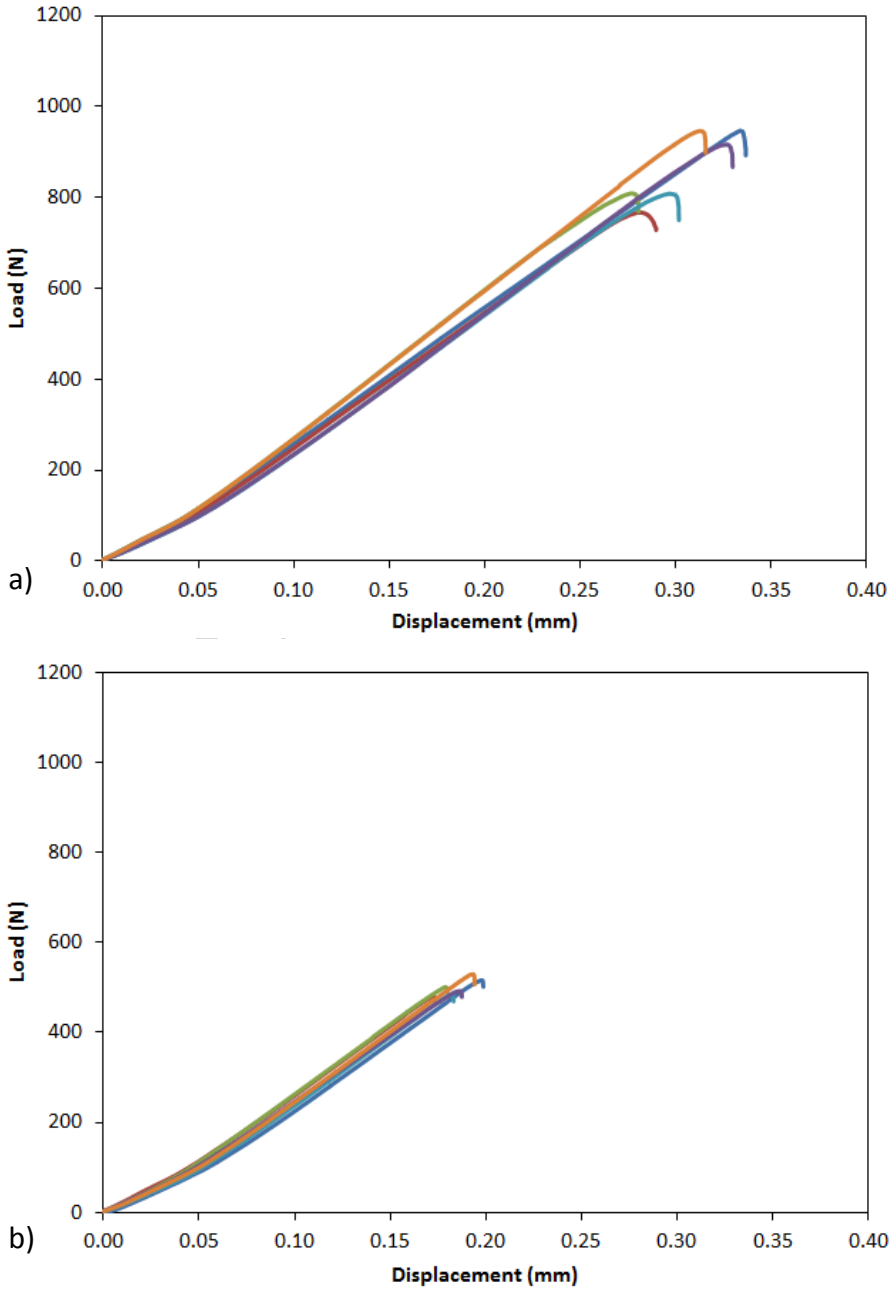

Figure 8. Load-displacement curves obtained in fracture toughness tests: a) granite; b) limestone.

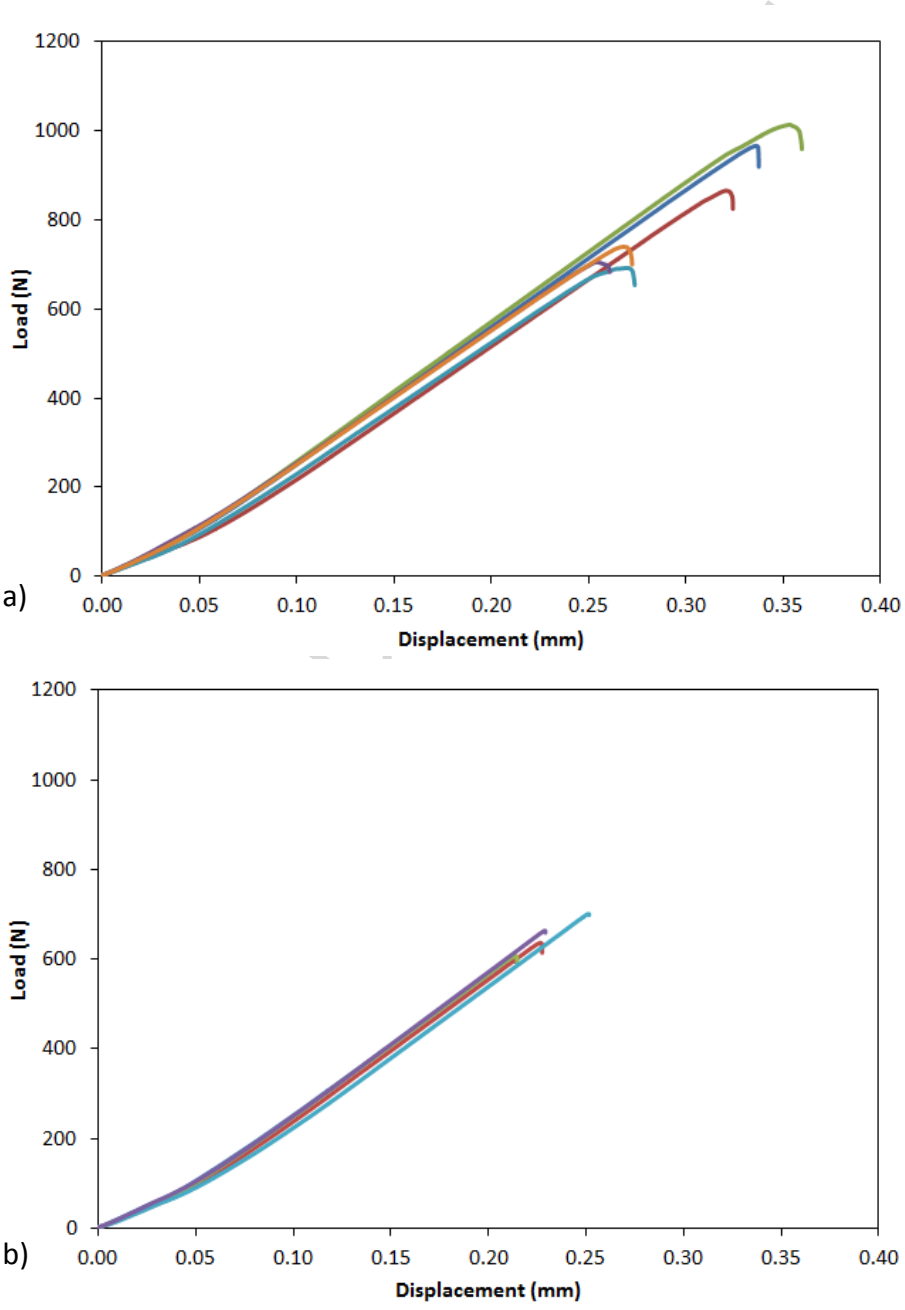

Figure 9. Load-displacement curves obtained in apparent fracture toughness tests (ρ=10 mm): a) granite; b) limestone.

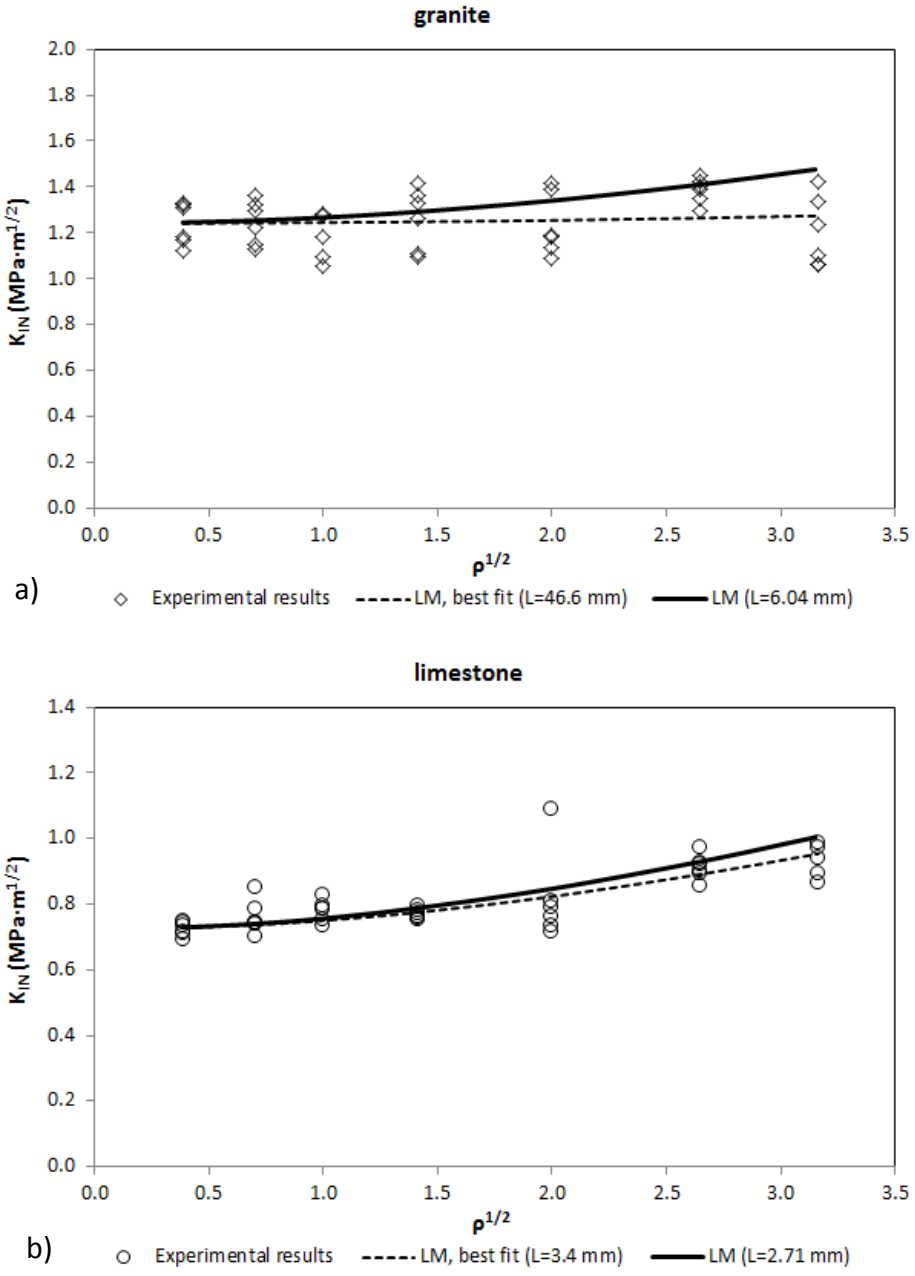

Figure 10. Fracture toughness and apparent fracture toughness experimental results, and comparison with the TCD (LM) predictions: a) granite; b) limestone.

Tables

Table 1. Some technical properties of the granite and limestone

	Granite	**Limestone**
Bulk density (kg/m^3)	2660	2540
Water absorption (%)	0.18	3.01
Abrasion resistance (mm)	19	22.5
Slip resistance (SRV)	73	42
Grain size (μm)	1000	800

Table 2. Compression and tensile properties of the granite and limestone. The results shown the average and the standard deviation

	Granite	**Limestone**
Compressive strength (MPa)	122.5 ± 4.8	135.7 ± 12.7
Elastic modulus, E_{50} (GPa)	45.6 ± 7.9	64.1 ± 2.2
Tensile strength (MPa)	9.0 ± 1.3	7.8 ± 1.1

Table 3. Results of fracture toughness tests.

Specimen (granite)	**K_{IC} (MPam$^{1/2}$)**	**Specimen (limestone)**	**K_{IC} (MPam$^{1/2}$)**
G-0-1	1.33	L-0-1	0.75
G-0-2	1.12	L-0-2	0.74
G-0-3	1.17	L-0-3	0.71
G-0-4	1.18	L-0-4	0.71
G-0-5	1.32	L-0-5	0.69
G-0-6	1.31	L-0-6	0.73

Table 4. Results of apparent fracture toughness tests.

Specimen (granite)	Notch radius (mm)	K_{IN} ($MPam^{1/2}$)	Specimen (limestone)	Notch radius (mm)	K_{IN} ($MPam^{1/2}$)
G-05-1	0.5	1.29	L-05-1	0.5	0.78
G-05-2		1.36	L-05-2		0.74
G-05-3		1.32	L-05-3		0.70
G-05-4		1.12	L-05-4		0.74
G-05-5		1.22	L-05-5		0.85
G-05-6		1.14	L-05-6		0.73
G-1-1	1.0	1.09	L-1-1	1.0	0.78
G-1-2		1.18	L-1-2		0.78
G-1-3		1.05	L-1-3		0.73
G-1-4		1.27	L-1-4		0.75
G-1-5		1.28	L-1-5		0.79
G-1-6		Not valid	L-1-6		0.82
G-2-1	2.0	1.36	L-2-1	2.0	0.75
G-2-2		1.10	L-2-2		0.79
G-2-3		1.09	L-2-3		0.76
G-2-4		1.41	L-2-4		0.78
G-2-5		1.32	L-2-5		0.77
G-2-6		1.26	L-2-6		0.75
G-4-1	4.0	1.09	L-4-1	4.0	1.09
G-4-2		1.18	L-4-2		0.76
G-4-3		1.13	L-4-3		0.73
G-4-4		1.18	L-4-4		0.71
G-4-5		1.41	L-4-5		0.78
G-4-6		1.38	L-4-6		0.80
G-7-1	7.0	1.29	L-7-1	7.0	0.90
G-7-2		1.34	L-7-2		0.92
G-7-3		1.45	L-7-3		0.85
G-7-4		1.38	L-7-4		0.92
G-7-5		1.42	L-7-5		0.89
G-7-6		1.40	L-7-6		0.97
G-10-1	10	1.33	L-10-1	10	0.94
G-10-2		1.23	L-10-2		0.89
G-10-3		1.42	L-10-3		0.86
G-10-4		1.06	L-10-4		0.97
G-10-5		1.06	L-10-5		0.98
G-10-6		1.10	L-10-6		Not valid

Research highlights:

- The notch effect is analysed in granite and limestone
- The Theory of Critical Distances is applied to fracture analysis of granite and limestone
- The corresponding critical distances are obtained
- Notch effect in limestone is noticeable, whereas it is very limited in granite